



HHS Public Access

Author manuscript

Brain Res. Author manuscript; available in PMC 2016 January 25.

Published in final edited form as:

Brain Res. 2008 July 30; 1222: 214–221. doi:10.1016/j.brainres.2008.05.058.

The Development of an Improved Preclinical Mouse Model of Intracerebral Hemorrhage Using Double Infusion of Autologous Whole Blood

Jian Wang, Jocelyn Fields, and Sylvain Doré

Department of Anesthesiology/Critical Care Medicine, Johns Hopkins University, Baltimore, Maryland

Abstract

The present study was conducted in mice to validate a double blood infusion model of intracerebral hemorrhage (ICH) that does not use anticoagulant. We investigated the effect of intrastriatal infusion of blood on hematoma volume, neurologic function, brain edema and swelling, and markers of neuroinflammation and oxidative DNA damage. Anesthetized C57BL/6 adult male mice were infused in the left striatum with 4 μ l of blood over 20 min at 0.2 μ l/min; the needle was left in place for 7 min, and the remaining 6 μ l of blood was then infused over 30 min. The injection needle was slowly withdrawn 20 min after the second injection. Sham-operated control mice received only needle insertion. The hematoma produced in this model was primarily restricted to the striatum, and the mice demonstrated severe neurologic deficits that appeared within 60 min and remained evident at 72 h. Brain water content and swelling were significantly increased and were associated with a marked increase in ICH-induced neutrophil infiltration, microglial/macrophage and astrocyte activation, cytochrome c release, and oxidative DNA damage. Other groups have mixed the anticoagulant heparin with the infused blood, an agent that could affect in vivo clot formation. We believe that this double blood infusion model that does not use anticoagulant improves upon the procedure and provides an easy and reproducible alternative for inducing ICH in mice; it should be useful for studying the pathophysiology of ICH and for testing potential pharmaceutical and surgical interventions.

Keywords

Blood; Brain edema; Hemispheric enlargement; Inflammation; Reactive oxygen species; Stroke

Address correspondence to: Jian Wang, MD, PhD, Department of Anesthesiology/Critical Care Medicine, Johns Hopkins University, School of Medicine, 720 Rutland Ave, Traylor Bldg 809, Baltimore, MD 21205 (Phone: 410.955.3640; Fax: 410.502.5177; jwang79@jhmi.edu). Or: Sylvain Doré, PhD, Department of Anesthesiology/Critical Care Medicine, Johns Hopkins University, School of Medicine, 720 Rutland Ave, Ross 365, Baltimore, MD 21205 (Phone: 410.614.4859; Fax: 410.955.7271; sdore@jhmi.edu; www.hopkinsmedicine.org/dorelab).

Publisher's Disclaimer: This is a PDF file of an unedited manuscript that has been accepted for publication. As a service to our customers we are providing this early version of the manuscript. The manuscript will undergo copyediting, typesetting, and review of the resulting proof before it is published in its final citable form. Please note that during the production process errors may be discovered which could affect the content, and all legal disclaimers that apply to the journal pertain.

1. Introduction

Intracerebral hemorrhage (ICH) is one of the most lethal stroke subtype (Mayer and Rincon, 2006; Wang and Dore, 2007b). Mortality reaches 50% and disability in survivors is common. In comparison to ischemic stroke, pathologic mechanisms of ICH-induced brain injury remain relatively unclear, although recent preclinical studies have identified that neuroinflammation (glial activation and neutrophil infiltration), oxidative stress, proteases, red blood cell lysis, and thrombin may play a role (Ardizzone, et al., 2007; Rosenberg, 2002; Wang and Dore, 2007a; Wang and Dore, 2007b; Wang, et al., 2003; Wang and Tsirka, 2005b; Xi, et al., 2006; Xue, et al., 2006). Therefore, optimized, reproducible, and controllable preclinical models of ICH are vital for studying gene products and signaling pathways that may be involved in the cascade of events that lead to ICH-induced brain injury as well as for testing potential pharmaceutical and surgical interventions.

Several animal models of ICH have been developed in the rodent, cat, rabbit, dog, pig, and primate (reviewed in Andaluz, et al., 2002; Wang and Dore, 2007b). Of those, laboratory mice are most useful because they are more economical and relatively more homogeneous within strains than larger animals. In addition, genetically modified mice are reliable tools to study particular gene/protein functions in the pathophysiology of ICH. Techniques such as injection of collagenase or blood into the mouse brain parenchyma have been established after being used in larger animals. Local injection of recombinant collagenase to induce intracerebral bleeding has been widely used in mice (Wang and Dore, 2007b). The hemorrhage in this model is highly reproducible, with hematoma developing within 5 h (Wang and Dore, 2007a). Furthermore, it replicates the primary vascular rupture; the resulting bleed is spontaneous in nature, mimicking clinical ICH. A drawback of this model is the presence of bacterial collagenase, which is thought by some to enhance inflammation and therefore affect ICH outcomes in subtle ways.

Compared with the collagenase model, the blood infusion model is more useful for studying the pathophysiology and biochemical events that result from the presence of blood in the brain tissue. Intracerebral blood infusion models that use donor or autologous whole blood have recently been developed in mice (Table 1). Belayev et al. (2003) developed a mouse model in which heparinized donor blood is infused into the striatum. Nakamura et al. (2004) first reported the development of an autologous blood infusion model, but did not specify whether anticoagulant was used. Rynkowski et al. (2008) established a mouse model using double infusion of heparinized autologous blood. Other groups have used single blood infusion instead of double blood infusion to create a hematoma within the mouse striatum with or without the use of anticoagulant heparin (Lee, et al., 2006; Qu, et al., 2007; Tejima, et al., 2007; Xue, et al., 2006; Zhao, et al., 2007). However, drawbacks of current blood infusion models include: lack of primary vascular rupture; variable lesion size due to backflow of the injected blood or ventricular rupture; potential effects of donor blood or anticoagulant on inflammation, complement, or the coagulation system. In addition, the technique of blood infusion in mice remains challenging given the relatively small volume of blood that can be injected into the brain.

In view of the pitfalls and shortcomings of the current blood infusion models, our goal was to validate a modified double blood infusion model in mice that does not use anticoagulant and assess hematoma volume, neurological function, brain edema and swelling, neuroinflammation, and oxidative damage.

2. Results

In this blood-induced ICH model, we infused 10 μl of autologous whole blood at a very slow, controlled rate (0.2 $\mu\text{l}/\text{min}$) into the left striatum in two stages. This revised method of ICH induction is based on recent evidence that clot formation in humans is a gradual process (Brott, et al., 1997; Kazui, et al., 1996). In the pilot cohort study, we tried to infuse 20–30 μl of autologous blood into the striatum at an infusion rate of 2–3 $\mu\text{l}/\text{min}$, but frequently observed substantial backflow of blood during and after the infusion. Such backflow resulted in large variations in hematoma volume. In previous studies, we did not observe backflow when we injected collagenase into mouse brains at a rate of 0.1 $\mu\text{l}/\text{min}$ (Wang and Dore, 2007a; Wang, et al., 2007); therefore, to prevent backflow in the current study, we modified the method of blood infusion by reducing the speed of injection and infusing the blood in two stages. We found that double infusion of a small volume of blood (10 μl) at 0.2 $\mu\text{l}/\text{min}$ significantly reduced the backflow and extravasation of blood along the needle track. The method generated reproducible hematoma volumes without subarachnoid blood accumulation and prevented nonphysiologic pressure injury to adjacent brain tissue, thus mimicking the natural bleeding process closely. The hematoma produced in this model was consistent in regard to location and volume and caused reproducible and reliable neurologic deficits. The typical morphology of hematoma at 72 h after blood infusion is shown in Fig. 1. The hematoma was largely restricted to the striatum, with some blood pooled within the corpus callosum. Extension of the hematoma to the intraventricular or subarachnoid spaces was not observed on the histologic brain slices from any animal.

2.1. Hematoma volume and neurologic function

Histologic examination of the brain after 72 h survival revealed the presence of a localized hematoma lesion in all animals subjected to blood infusion, whereas in the sham-operated mice, only the needle track without any hematoma was visible (Fig. 2A). The brain injury volume calculated from serial sections via an image analysis system was $2.31 \pm 0.87 \text{ mm}^3$ for the ICH group and 0.21 ± 0.03 for the sham group (Fig. 2B, $n = 7/\text{group}$, $p < 0.001$).

All mice subjected to blood infusion began to exhibit neurologic deficits within 60 min, deteriorated gradually, and were maximally impaired at 24 h; deficits remained evident 72 h after ICH induction. Sham-operated control mice demonstrated minimal neurologic deficits at all time points examined (Fig. 2C, $n = 8/\text{group}$, all $p < 0.001$).

2.2. Brain edema and swelling

Brain edema following ICH usually peaks on the third day (Wang and Tsirka, 2005b; Wasserman and Schlichter, 2007a; Xi, et al., 2006). Here, we first examined the brain water content as a means to measure brain edema formation in this ICH model. The results showed that the infusion of 10 μl blood into the left striatum produced significant increases in brain

water content in the ipsilateral basal ganglia at 72 h ($78.82 \pm 0.56\%$ vs. $77.02 \pm 2.62\%$, $n = 6/\text{group}$, $p < 0.01$); however, brain water content in the ipsilateral cortex was not increased, as the hematoma was restricted primarily in the striatum in our model (Fig. 3A).

We next measured the percentage of hemispheric enlargement to evaluate brain swelling, which is a reflection of overall edema. It is also believed to be responsible for much of the brain damage and death that results from severe stroke. The hemispheric enlargement was quantified by digitizing serial brain sections and calculating the cumulative area. We found that hemispheric enlargement was significantly greater in the ICH group ($8.81 \pm 2.06\%$) than in the sham group ($0.19 \pm 0.74\%$; Fig. 3B, $n = 6/\text{group}$, $p < 0.001$).

2.3. Neuroinflammatory markers

2.3.1. Infiltration of neutrophils—Neutrophil infiltration occurs following experimental ICH induced by autologous blood (Gong, et al., 2000; Xue and Del Bigio, 2000) or collagenase injection (Wang and Dore, 2007a; Wang and Dore, 2007b; Wang and Tsirka, 2005b). We investigated here whether it also occurs in this autologous blood-induced model. As indicated by immunoreactivity of myeloperoxidase (MPO), double blood infusion produced a robust infiltration of neutrophils into the affected striatum at 72 h after ICH; no MPO-immunoreactive neutrophils were observed in the striatum of sham-operated control mice (Fig. 4A, $n = 6/\text{group}$).

2.3.2. Activation of microglia—Microglia/macrophage activation also occurs following experimental ICH induced by autologous blood (Gong, et al., 2000; Xue and Del Bigio, 2000) or collagenase (Wang and Dore, 2007b; Wang and Tsirka, 2005a) and contributes to ICH-induced early brain injury (Aronowski and Hall, 2005; Wang and Dore, 2007a). To examine microglia/macrophage activation in this autologous blood-induced model, we used immunofluorescence staining of Iba1, a marker for microglia/macrophages (Ito, et al., 2001). After ICH, activated microglia/macrophages were characterized as cells with a spherical, amoeboid, or rod-like appearance and a cell body usually more than $7.5 \mu\text{m}$ in diameter, with short, thick processes and intense immunoreactivity. Resting microglia were characterized by small cell bodies ($<7.5 \mu\text{m}$ in diameter), long processes, and weak immunoreactivity. By using a combination of morphological criteria and a cell body diameter cutoff of $7.5 \mu\text{m}$, microglia/macrophages were classified as either resting or activated (Batchelor, et al., 1999; Rogove, et al., 2002; Wang and Dore, 2007a). Our results showed that activated microglia/macrophages were present in the striatum around the injury site 72 h after ICH and that resting microglia/macrophages were distributed sparsely in the striatum of sham-operated control mice (Fig. 4B, $n = 6/\text{group}$).

2.3.3 Activation of astrocytes—Astrocytes react to many central nervous system challenges/insults, and reactive astrocytes are a hallmark of various neuropathologic conditions (Anderson, et al., 2003; Miller, 2005). To examine astrocytic reaction in this autologous blood infusion model, we used glial fibrillary acidic protein (GFAP) immunofluorescence labeling because reactive astrocytes exhibit striking intensification of GFAP immunoreactivity and increases in the number, length, and thickness of GFAP-positive processes. Increased GFAP immunoreactivity was observed in the striatum around

the injury site 72 h after ICH; resting (nonreactive) astrocytes with small cell bodies, fine terminal processes, and weak immunoreactivity were observed in the striatum of the sham-operated control mice (Fig. 4C, $n = 6/\text{group}$).

2.4. Cytochrome c release and oxidative DNA damage

Release of mitochondrial cytochrome c has been linked to apoptotic cell death (Garrido, et al., 2006), a significant contributor to ICH-induced brain damage (Matsushita, et al., 2000; Qureshi, et al., 2003; Wang, et al., 2003). In addition, several groups have shown increased cytochrome c release following ICH (Felberg, et al., 2002; Wang, et al., 2007) and cerebral ischemia (Li, et al., 2004; Shichinohe, et al., 2004). To examine cytochrome c release in this autologous blood infusion model, immunofluorescence labeling of cytochrome c was conducted. Here, intense immunoreactivity of cytosolic cytochrome c was detected in the striatum around the injury site 72 h after ICH; in contrast, we did not detect any enhanced cytochrome c immunoreactivity in the cells around the border region of injury in sham-operated control mice (Fig. 5A, $n = 6/\text{group}$).

Oxidative damage contributes to ICH-induced early brain injury (Wang and Dore, 2007b). To examine oxidative DNA damage in this blood infusion model, we used immunofluorescence staining of 8-hydroxyguanosine (8-OHG), a commonly used biomarker for oxidative DNA damage caused by superoxide anion (Kim, et al., 2001; Nakamura, et al., 2005; Wang and Dore, 2007a). Here, increased immunoreactivity of 8-OHG was observed in the striatum around the injury site 72 h after ICH, but was not observed in the striatum of sham-operated control mice (Fig. 5B, $n = 6/\text{group}$).

3. Discussion

In the present study, we validated a modified double autologous blood infusion model in mice that does not require anticoagulant. We found that the hematoma produced in this model was primarily restricted to the striatum. Mice subjected to blood infusion developed severe neurologic deficits, which appeared within 60 min and remained evident at 72 h after ICH. Brain water content and swelling were significantly increased and were associated with a marked increase in ICH-induced neutrophil infiltration, microglial/macrophage and astrocyte activation, cytochrome c release, and oxidative DNA damage.

Compared with previously published mouse blood infusion models (Table 1), the current model has several advantages. First, we used a two-stage infusion of a small volume of blood (10 μl) with a very slow and controlled infusion rate (0.2 $\mu\text{l}/\text{min}$), which significantly reduces the backflow and extravasation of blood along the needle track to ventricular and/or subarachnoid spaces, prevents nonphysiologic pressure injury to adjacent brain tissue, and mimics the natural bleeding process more closely. The hematoma produced in this model was consistent in regard to location and volume and caused more persistent and reliable neurologic deficits. Based on our experience and accumulated preliminary results, we have noticed that neurologic deficits resulting from this modified blood infusion model usually correlate much better with brain injury volume than that of the single blood infusion model (data not shown). Second, we used autologous whole blood, which excludes the influence of donor blood on the complement system and inflammation. Third, we did not add

anticoagulant to the blood, thus preventing the potential influence on the coagulation system and in vivo clot formation. In addition, the body temperature was maintained at $37.0 \pm 0.5^{\circ}\text{C}$ throughout the experimental and recovery periods to minimize the potential influence of temperature fluctuations (MacLellan and Colbourne, 2005). Finally, to minimize leukocytosis and activation of complement, blood was harvested slowly, and the tail was not rubbed.

Evidence suggests that enhanced neuroinflammation and oxidative damage are associated with ICH-induced early brain injury (Wang and Dore, 2007b; Wasserman and Schlichter, 2007b; Xi, et al., 2006), most likely due to the accumulation of free heme within the brain. Free heme is a potent pro-oxidant and a strong inducer of inflammation (Wagener, et al., 2001; Wagner, et al., 2003; Wang and Dore, 2007a). It is mainly released from red blood cells that leak during hemorrhage or through the damaged blood-brain barrier and hemolysis of hemoglobin. It is also released from other cellular components of brain tissue. A large accumulation of free heme following hemorrhage could result in increased vasopermeability, vasoreactivity, oxidative damage, and tissue infiltration of leukocytes (Wagener, et al., 2001; Wagner, et al., 2003).

The present data demonstrated that C57BL/6 mice subjected to double blood infusion have enhanced neutrophil infiltration and activation of microglia/macrophages and astrocytes. Our observations are also supported by the work of other groups, who used an autologous blood infusion model in rats (Gong, et al., 2000; Xue and Del Bigio, 2000). Following ICH, infiltrating leukocytes, activated microglia/macrophages, and reactive astrocytes could damage brain tissues by increasing vascular permeability, releasing proinflammatory proteases, and generating reactive oxygen species (ROS) (Eder, 2005; Facchinetti, et al., 1998; Tejima, et al., 2007; Wang and Tsirka, 2005a; Weiss, 1989). ROS can trigger cytochrome c release from mitochondria into the cytosol, which is often followed by DNA damage and cell death (Matz, et al., 2001). Therefore, cytochrome c release can be used as a means of predicting cell death (Garrido, et al., 2006). Consistent with the results from an autologous blood infusion model in rat (Nakamura, et al., 2005) and our collagenase-induced model in mice (Wang and Dore, 2007a; Wang, et al., 2007), we observed significantly increased cytosolic cytochrome c and 8-OHG immunoreactivity 72 h after blood infusion. Associated with the increased neuroinflammation and oxidative damage, we also observed significantly increased brain edema and swelling.

In conclusion, the double blood infusion model of ICH presented here will enable researchers to mimic the clinical ICH more closely than has been possible with other mouse models. Infusion of 10 μl blood into the striatum at 0.2 $\mu\text{l}/\text{min}$ produced a consistent hematoma restricted primarily to the striatum. In addition, mice developed a significant increase in brain edema and swelling, severe neurologic deficits, neuroinflammation, oxidative DNA damage, and cytochrome c release. We believe that this anticoagulant-free, modified double blood infusion model could be easier to use and more reproducible for inducing ICH in mice than previously reported models. It can provide a better alternative for studying gene products and signaling pathways that may be involved in the cascade of events leading to ICH-induced brain injury and for testing potential pharmaceutical and surgical interventions.

4. Experimental procedures

4.1 Animals

This study was conducted in accordance with the National Institutes of Health guidelines for the use of experimental animals. Experimental protocols were approved by the Johns Hopkins University Animal Care and Use Committee. Adequate measures were taken to minimize the number of laboratory mice used and to ensure minimal pain or discomfort in mice. Adult male C57BL/6 mice (24–30 g, 10–12 weeks old) were obtained from our colonies.

4.2 Double blood infusion model

For each separate study, age- and weight-matched C57BL/6 mice were randomly allocated into two groups: an ICH group and a needle insertion only group (sham). Mice were anesthetized by halothane (3% initial, 1% to 1.5% maintenance) in O₂ and air (80%:20%) and placed in a stereotaxic frame (Stoelting Co., Wood Dale, IL). A midline scalp incision was made and a hole was drilled in the left side of the skull (0.6 mm anterior and 2.0 mm lateral of the bregma) in preparation for the infusion. The mouse tail was immersed in warm water for 2 min and cleaned with 70% ethanol; then, 0.8 cm of the tail tip was cut off with a pair of sterile surgical scissors. We did not attempt to increase blood flow by rubbing the tail, as this will result in leukocytosis (increased white blood cell count) and increase the risk of tissue fluid contamination. Blood (10 µl) was collected slowly (to minimize activation of complement) into a sterile 10-µl Hamilton syringe without the use of an anticoagulant. After blood collection, pressure was applied or a cauterizing agent (e.g., silver nitrate) was used to stop the bleeding. Within 1 min of blood collection, the Hamilton syringe was secured onto a motorized microinjector (Stoelting) set to inject at 0.2 µl/min. The 26-gauge needle attached to the Hamilton syringe was stereotaxically inserted into the striatum 3.8 mm below the surface of the skull. First, 4 µl of blood was infused over 20 min; the needle was left in place for another 7 min, and the remaining 6 µl of blood was infused over 30 min. The needle was slowly withdrawn 20 min after the second injection to minimize backflow. The burr hole in the skull was sealed with bone wax (ETHICON, Piscataway, NJ), and the scalp incision was closed with Super glue (Henkel Consumer Adhesive, Inc., Avon, OH). Body temperature was maintained at 37.0 ± 0.5°C throughout the experimental and recovery periods with a rectal probe; animals regained consciousness within 10 min. Control mice received only needle insertion into the left striatum. None of the mice died during the study before the endpoints of the experiment.

4.3 Neurologic deficit

An investigator blinded to the experimental cohort scored all mice (8 sham; 8 ICH) for neurologic deficits with a 24-point neurologic scoring system (Wang, et al., 2006) 4, 24, 48, and 72 h after blood infusion. The tests included body symmetry, gait, climbing, circling behavior, front limb symmetry, and compulsory circling. Each test was graded from 0 to 4, establishing a maximum deficit score of 24. Immediately after the testing at 72 h, the mice were sacrificed for immunofluorescence analysis.

4.4 Hemorrhagic injury analysis

All processing and analysis of tissue sections as described in this and the following sections were conducted by an observer blind to the experimental cohort. Sham and ICH mice ($n = 7$ /group) were euthanized, and their brains were harvested, fixed in 4% paraformaldehyde for 24 h, and cryoprotected in serial phosphate-buffered sucrose solutions (20, 30, and 40%) at 4°C. Then the brains were cut into 30- μ m sections with a cryostat. Sections were stained with Luxol fast blue and Cresyl Violet (Wang, et al., 2003; Wang and Tsirka, 2005c) before being quantified for injury area with SigmaScan Pro software (version 5.0.0 for Windows; Systat, Port Richmond, CA). The injured hemorrhagic areas on six coronal slices from different levels of the brain were summed, and the volumes in cubic millimeters were calculated by multiplying the thickness by the measured areas (Wang, et al., 2003; Wang and Tsirka, 2005c).

4.5 Brain water content

Brain edema was assessed by measuring brain water content as described previously with minor modifications (Wang and Tsirka, 2005b; Wang and Tsirka, 2005c). Briefly, mice ($n = 6$ /group) were sacrificed by decapitation 72 h after blood infusion. The brains were removed immediately and divided into five parts: ipsilateral and contralateral basal ganglia, ipsilateral and contralateral cortex, and cerebellum (which served as an internal control). Brain samples were weighed immediately on an analytical balance (Denver Instrument Co, Denver, CO) to obtain the wet weight and then dried at 100°C for 48 h to obtain the dry weight. Brain edema was expressed as $(\text{wet weight} - \text{dry weight})/\text{wet weight of brain tissue} \times 100$.

4.6 Hemispheric enlargement

Brain edema was further measured by percentage of hemispheric enlargement at 72 h after blood infusion. Mice ($n = 6$ /group) were euthanized, and their brains were harvested, and rapidly frozen at -80°C. Frozen brain sections taken at 500 μ m intervals by cryostat were stained with Luxol fast blue/Cresyl violet according to a published protocol (Geisler, et al., 2002). The areas of ipsilateral hemisphere and contralateral hemisphere were analyzed with advanced SPOT image software (Diagnostic Instruments Inc., Sterling Heights, MI). The volumes of ipsilateral and contralateral hemispheres were calculated by multiplying each area by the distance between sections. Hemisphere enlargement (%) was expressed as $[(\text{ipsilateral hemisphere volume} - \text{contralateral hemisphere volume})/\text{contralateral hemisphere volume}] \times 100$ (Kondo, et al., 1997; Manley, et al., 2000).

4.7 Immunofluorescence

Mice were anesthetized by intraperitoneal injection with Avertin (2-2-2 tribromoethanol; Sigma, St. Louis, MO; 0.5 mg/g body weight) and perfused transcardially with phosphate-buffered saline (PBS, pH 7.4) for 5 min and then with ice-cold 4% paraformaldehyde in PBS for another 5 min. Sham-operated control mice were perfused similarly. The brains were harvested, fixed in 4% paraformaldehyde for 24 h, and cryoprotected in serial phosphate-buffered sucrose solutions (20, 30, and 40%) at 4°C. Then the brains were cut into 12- μ m sections with a cryostat.

Immunofluorescence was carried out as described previously (Wang and Dore, 2007a; Wang and Tsirka, 2005b; Wang and Tsirka, 2005c). Briefly, free-floating sections were washed in PBS for 20 min, blocked in 5% normal goat serum, and incubated overnight at 4°C with one of the following primary antibodies: rabbit anti-MPO (neutrophil marker; 1:100; DAKO, UK); rabbit anti-Iba 1 (microglia marker; 1:1000; Wako Chemicals, Richmond, VA); rabbit anti-GFAP (astrocyte marker; 1:1000; DakoCytomation, Copenhagen, Denmark); mouse anti-8-OHG (10 µg/ml, Oxis International Inc, Portland, OR); mouse anti-cytochrome c (1:1000; BD Pharmingen, San Diego, CA). Sections were then incubated with Alexa 488 (1:1000; Molecular Probes)- or Cy3 (1:1000; Jackson ImmunoResearch, West Grove, PA)-conjugated secondary antibody. Control sections were processed by the same method, except that primary antibodies were omitted. Stained sections were examined with a fluorescence microscope (ECLIPSE TE2000-E, Nikon, Japan).

4.8 Statistics

All data are expressed as means \pm SD. Differences between two groups were determined by two-tailed Student's *t*-test. Neurologic scores between ICH and sham groups at different time points were analyzed by two-way ANOVA followed by Bonferroni correction. Statistical significance was set at $p < 0.05$.

Acknowledgments

This work was supported by an AHA-SDG 0630223N (JW) and NIH grants AG022971 and NS046400 (SD). We thank all members of the Doré lab for helpful discussions and Claire Levine for assistance with this manuscript.

Abbreviations

8-OHG	8-hydroxyguanosine
GFAP	Glial fibrillary acidic protein
ICH	intracerebral hemorrhage
MPO	myeloperoxidase
ROS	reactive oxygen species

References

- Andaluz N, Zuccarello M, Wagner KR. Experimental animal models of intracerebral hemorrhage. *Neurosurg Clin N Am.* 2002; 13:385–393. [PubMed: 12486927]
- Anderson MF, Blomstrand F, Blomstrand C, Eriksson PS, Nilsson M. Astrocytes and stroke: networking for survival? *Neurochem Res.* 2003; 28:293–305. [PubMed: 12608702]
- Ardizzone TD, Zhan X, Ander BP, Sharp FR. SRC kinase inhibition improves acute outcomes after experimental intracerebral hemorrhage. *Stroke.* 2007; 38:1621–1625. [PubMed: 17395859]
- Aronowski J, Hall CE. New horizons for primary intracerebral hemorrhage treatment: experience from preclinical studies. *Neurol Res.* 2005; 27:268–279. [PubMed: 15845210]
- Batchelor PE, Liberatore GT, Wong JY, Porritt MJ, Frerichs F, Donnan GA, Howells DW. Activated macrophages and microglia induce dopaminergic sprouting in the injured striatum and express brain-derived neurotrophic factor and glial cell line-derived neurotrophic factor. *J Neurosci.* 1999; 19:1708–1716. [PubMed: 10024357]

- Belayev L, Saul I, Curbelo K, Busto R, Belayev A, Zhang Y, Riyamongkol P, Zhao W, Ginsberg MD. Experimental intracerebral hemorrhage in the mouse: histological, behavioral, and hemodynamic characterization of a double-injection model. *Stroke*. 2003; 34:2221–2227. [PubMed: 12920264]
- Brott T, Broderick J, Kothari R, Barsan W, Tomsick T, Sauerbeck L, Spilker J, Duldner J, Khoury J. Early hemorrhage growth in patients with intracerebral hemorrhage. *Stroke*. 1997; 28:1–5. [PubMed: 8996478]
- Eder C. Regulation of microglial behavior by ion channel activity. *J Neurosci Res*. 2005; 81:314–321. [PubMed: 15929071]
- Facchinetti F, Dawson VL, Dawson TM. Free radicals as mediators of neuronal injury. *Cell Mol Neurobiol*. 1998; 18:667–682. [PubMed: 9876873]
- Felberg RA, Grotta JC, Shirzadi AL, Strong R, Narayana P, Hill-Felberg SJ, Aronowski J. Cell death in experimental intracerebral hemorrhage: the "black hole" model of hemorrhagic damage. *Ann Neurol*. 2002; 51:517–524. [PubMed: 11921058]
- Garrido C, Galluzzi L, Brunet M, Puig PE, Didelot C, Kroemer G. Mechanisms of cytochrome c release from mitochondria. *Cell Death Differ*. 2006; 13:1423–1433. [PubMed: 16676004]
- Geisler S, Heilmann H, Veh RW. An optimized method for simultaneous demonstration of neurons and myelinated fiber tracts for delineation of individual trunco- and palliothalamic nuclei in the mammalian brain. *Histochem Cell Biol*. 2002; 117:69–79. [PubMed: 11819099]
- Gong C, Hoff JT, Keep RF. Acute inflammatory reaction following experimental intracerebral hemorrhage in rat. *Brain Res*. 2000; 871:57–65. [PubMed: 10882783]
- Ito D, Tanaka K, Suzuki S, Dembo T, Fukuuchi Y. Enhanced expression of Iba1, ionized calcium-binding adapter molecule 1, after transient focal cerebral ischemia in rat brain. *Stroke*. 2001; 32:1208–1215. [PubMed: 11340235]
- Kazui S, Naritomi H, Yamamoto H, Sawada T, Yamaguchi T. Enlargement of spontaneous intracerebral hemorrhage: incidence and time course. *Stroke*. 1996; 27:1783–1787. [PubMed: 8841330]
- Kim GW, Lewen A, Copin J, Watson BD, Chan PH. The cytosolic antioxidant, copper/zinc superoxide dismutase, attenuates blood-brain barrier disruption and oxidative cellular injury after photothrombotic cortical ischemia in mice. *Neuroscience*. 2001; 105:1007–1018. [PubMed: 11530238]
- Kondo T, Reaume AG, Huang TT, Carlson E, Murakami K, Chen SF, Hoffman EK, Scott RW, Epstein CJ, Chan PH. Reduction of CuZn-superoxide dismutase activity exacerbates neuronal cell injury and edema formation after transient focal cerebral ischemia. *J Neurosci*. 1997; 17:4180–4189. [PubMed: 9151735]
- Lee JC, Cho GS, Choi BO, Kim HC, Kim YS, Kim WK. Intracerebral hemorrhage-induced brain injury is aggravated in senescence-accelerated prone mice. *Stroke*. 2006; 37:216–222. [PubMed: 16322488]
- Li F, Omori N, Hayashi T, Jin G, Sato K, Nagano I, Shoji M, Abe K. Protection against ischemic brain damage in rats by immunophilin ligand GPI-1046. *J Neurosci Res*. 2004; 76:383–389. [PubMed: 15079867]
- MacLellan CL, Colbourne F. Mild to moderate hyperthermia does not worsen outcome after severe intracerebral hemorrhage in rats. *J Cereb Blood Flow Metab*. 2005; 25:1020–1029. [PubMed: 15744245]
- Manley GT, Fujimura M, Ma T, Noshita N, Filiz F, Bollen AW, Chan P, Verkman AS. Aquaporin-4 deletion in mice reduces brain edema after acute water intoxication and ischemic stroke. *Nat Med*. 2000; 6:159–163. [PubMed: 10655103]
- Matsushita K, Meng W, Wang X, Asahi M, Asahi K, Moskowitz MA, Lo EH. Evidence for apoptosis after intercerebral hemorrhage in rat striatum. *J Cereb Blood Flow Metab*. 2000; 20:396–404. [PubMed: 10698078]
- Matz PG, Fujimura M, Lewen A, Morita-Fujimura Y, Chan PH. Increased cytochrome c-mediated DNA fragmentation and cell death in manganese-superoxide dismutase-deficient mice after exposure to subarachnoid hemolysate. *Stroke*. 2001; 32:506–515. [PubMed: 11157190]
- Mayer SA, Rincon F. Ultra-early hemostatic therapy for acute intracerebral hemorrhage. *Semin Hematol*. 2006; 43:S70–S76. [PubMed: 16427389]

- Miller G. Neuroscience. The dark side of glia. *Science*. 2005; 308:778–781. [PubMed: 15879185]
- Nakamura T, Keep RF, Hua Y, Hoff JT, Xi G. Oxidative DNA injury after experimental intracerebral hemorrhage. *Brain Res*. 2005; 1039:30–36. [PubMed: 15781043]
- Nakamura T, Xi G, Hua Y, Schallert T, Hoff JT, Keep RF. Intracerebral hemorrhage in mice: model characterization and application for genetically modified mice. *J Cereb Blood Flow Metab*. 2004; 24:487–494. [PubMed: 15129180]
- Qu Y, Chen-Roetling J, Benvenisti-Zarom L, Regan RF. Attenuation of oxidative injury after induction of experimental intracerebral hemorrhage in heme oxygenase-2 knockout mice. *J Neurosurg*. 2007; 106:428–435. [PubMed: 17367065]
- Qureshi AI, Suri MF, Ostrow PT, Kim SH, Ali Z, Shatla AA, Guterman LR, Hopkins LN. Apoptosis as a form of cell death in intracerebral hemorrhage. *Neurosurgery*. 2003; 52:1041–1047. discussion 1047–1048. [PubMed: 12699545]
- Rogove AD, Lu W, Tsirka SE. Microglial activation and recruitment, but not proliferation, suffice to mediate neurodegeneration. *Cell Death Differ*. 2002; 9:801–806. [PubMed: 12107823]
- Rosenberg GA. Matrix metalloproteinases in neuroinflammation. *Glia*. 2002; 39:279–291. [PubMed: 12203394]
- Rynkowski MA, Kim GH, Komotar RJ, Otten ML, Ducruet AF, Zacharia BE, Kellner CP, Hahn DK, Merkow MB, Garrett MC, Starke RM, Cho BM, Sosunov SA, Connolly ES. A mouse model of intracerebral hemorrhage using autologous blood infusion. *Nat Protoc*. 2008; 3:122–128. [PubMed: 18193028]
- Shichinohe H, Kuroda S, Abumiya T, Ikeda J, Kobayashi T, Yoshimoto T, Iwasaki Y. FK506 reduces infarct volume due to permanent focal cerebral ischemia by maintaining BAD turnover and inhibiting cytochrome c release. *Brain Res*. 2004; 1001:51–59. [PubMed: 14972653]
- Tejima E, Zhao BQ, Tsuji K, Rosell A, van Leyen K, Gonzalez RG, Montaner J, Wang X, Lo EH. Astrocytic induction of matrix metalloproteinase-9 and edema in brain hemorrhage. *J Cereb Blood Flow Metab*. 2007; 27:460–468. [PubMed: 16788715]
- Wagener FADTG, Eggert A, Boerman OC, Oyen WJG, Verhofstad A, Abraham NG, Adema G, van Kooyk Y, de Witte T, Figdor CG. Heme is a potent inducer of inflammation in mice and is counteracted by heme oxygenase. *Blood*. 2001; 98:1802–1811. [PubMed: 11535514]
- Wagner KR, Sharp FR, Ardizzone TD, Lu A, Clark JF. Heme and iron metabolism: role in cerebral hemorrhage. *J Cereb Blood Flow Metab*. 2003; 23:629–652. [PubMed: 12796711]
- Wang J, Dore S. Heme oxygenase-1 exacerbates early brain injury after intracerebral haemorrhage. *Brain*. 2007a; 130:1643–1652. [PubMed: 17525142]
- Wang J, Dore S. Inflammation after intracerebral hemorrhage. *J Cereb Blood Flow Metab*. 2007b; 27:894–908. [PubMed: 17033693]
- Wang J, Fields J, Zhao C, Langer J, Thimmulappa RK, Kensler TW, Yamamoto M, Biswal S, Dore S. Role of Nrf2 in protection against intracerebral hemorrhage injury in mice. *Free Radic Biol Med*. 2007; 43:408–414. [PubMed: 17602956]
- Wang J, Rogove AD, Tsirka AE, Tsirka SE. Protective role of tuftsin fragment 1–3 in an animal model of intracerebral hemorrhage. *Ann Neurol*. 2003; 54:655–664. [PubMed: 14595655]
- Wang J, Tsirka SE. Contribution of extracellular proteolysis and microglia to intracerebral hemorrhage. *Neurocrit Care*. 2005a; 3:77–85. [PubMed: 16159103]
- Wang J, Tsirka SE. Neuroprotection by inhibition of matrix metalloproteinases in a mouse model of intracerebral haemorrhage. *Brain*. 2005b; 128:1622–1633. [PubMed: 15800021]
- Wang J, Tsirka SE. Tuftsin fragment 1–3 is beneficial when delivered after the induction of intracerebral hemorrhage. *Stroke*. 2005c; 36:613–618. [PubMed: 15692122]
- Wang J, Zhuang H, Doré S. Heme oxygenase 2 is neuroprotective against intracerebral hemorrhage. *Neurobiol Dis*. 2006; 22:473–476. [PubMed: 16459095]
- Wasserman JK, Schlichter LC. Minocycline protects the blood-brain barrier and reduces edema following intracerebral hemorrhage in the rat. *Exp Neurol*. 2007a; 207:227–237. [PubMed: 17698063]
- Wasserman JK, Schlichter LC. Neuron death and inflammation in a rat model of intracerebral hemorrhage: effects of delayed minocycline treatment. *Brain Res*. 2007b; 1136:208–218. [PubMed: 17223087]

- Weiss SJ. Tissue destruction by neutrophils. *N Engl J Med.* 1989; 320:365–376. [PubMed: 2536474]
- Xi G, Keep RF, Hoff JT. Mechanisms of brain injury after intracerebral haemorrhage. *Lancet Neurol.* 2006; 5:53–63. [PubMed: 16361023]
- Xue M, Del Bigio MR. Intracerebral injection of autologous whole blood in rats: time course of inflammation and cell death. *Neurosci Lett.* 2000; 283:230–232. [PubMed: 10754230]
- Xue M, Hollenberg MD, Yong VW. Combination of thrombin and matrix metalloproteinase-9 exacerbates neurotoxicity in cell culture and intracerebral hemorrhage in mice. *J Neurosci.* 2006; 26:10281–10291. [PubMed: 17021183]
- Zhao X, Sun G, Zhang J, Strong R, Dash PK, Kan YW, Grotta JC, Aronowski J. Transcription factor Nrf2 protects the brain from damage produced by intracerebral hemorrhage. *Stroke.* 2007; 38:3280–3286. [PubMed: 17962605]



Fig. 1. Representative unstained mouse brain section obtained 72 h after infusion of 10 μ l autologous whole blood into the striatum. Blood was observed primarily in the striatum, with some blood pooled within the corpus callosum. Scale bar = 100 μ m.

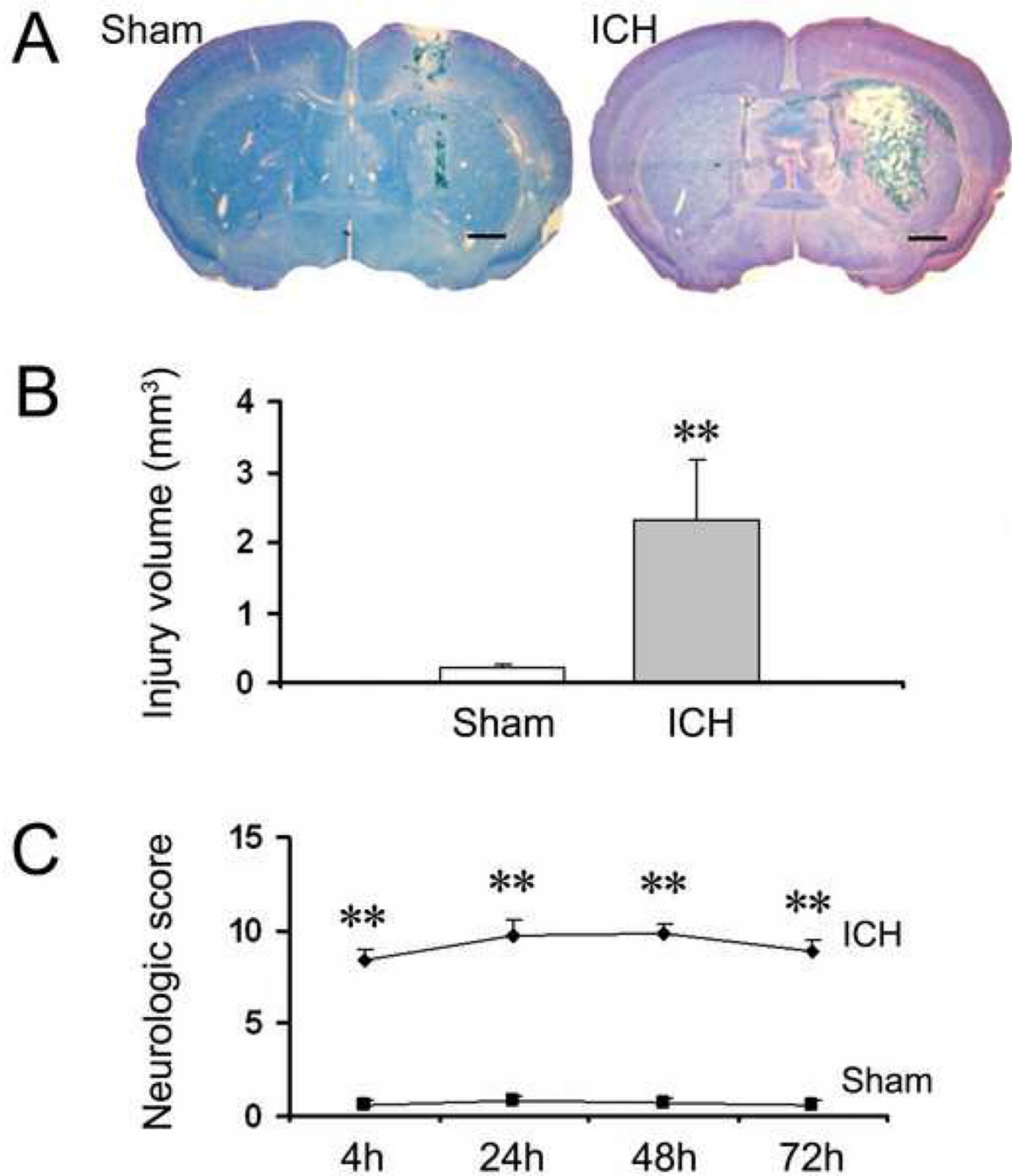


Fig. 2. The infusion of 10 μ l autologous whole blood into the striatum of mice produces extensive brain damage and severe neurologic deficits within 72 h. Age- and weight-matched C57BL/6 mice were randomly allocated into two groups: intracerebral hemorrhage group (ICH) and needle insertion only group (sham). (A) Representative brain sections obtained 72 h after the sham procedure (left) and intrastratial infusion of 10 μ l autologous whole blood (right). Brain sections were stained with Luxol fast blue/Cresyl Violet. Intrastratial infusion of 10 μ l blood produced extensive brain damage; whereas the sham procedure produced very

limited needle track damage. Scale bar = 100 μm . (B) Quantification shows significantly larger brain injury volume in the ICH group than in the sham group at 72 h ($n = 7/\text{group}$, $**p < 0.001$). (C) An investigator blinded to the experimental cohort assessed the neurologic deficits of mice with a 24-point neurologic scoring system at 4, 24, 48, and 72 h. Neurologic deficits were significantly more severe in the ICH group than in the sham group ($n = 8/\text{group}$, $**p < 0.001$). Values are means \pm SD.

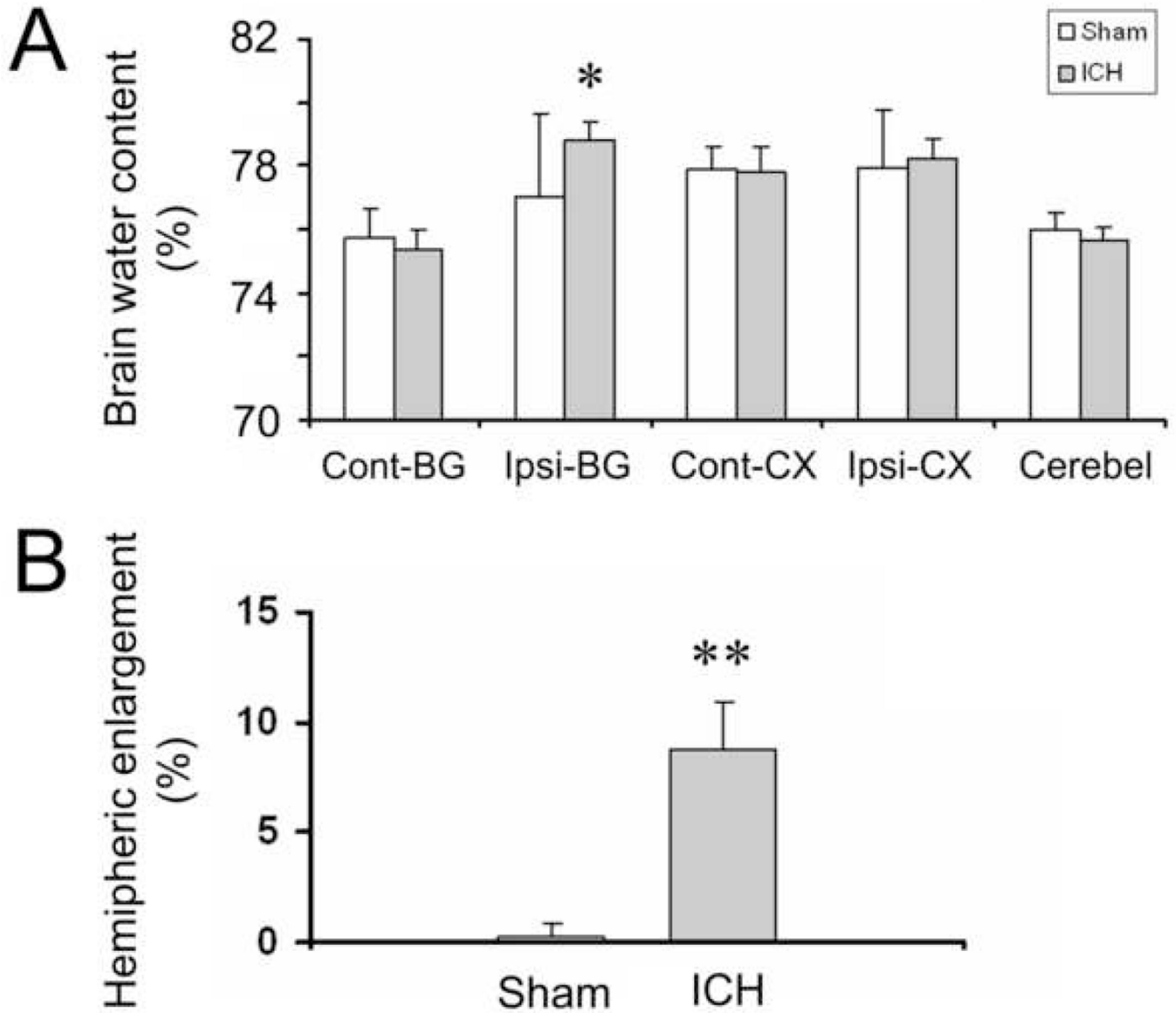


Fig. 3.

The infusion of 10 μ l autologous whole blood into the striatum of mice produces significant increases in brain edema and swelling at 72 h. Age- and weight-matched C57BL/6 mice were randomly allocated into two groups: intracerebral hemorrhage group (ICH) and needle insertion only group (sham). (A) Seventy-two hours after infusion of blood, brain water content in the ipsilateral basal ganglia (Ipsi-BG) of the ICH group was significantly higher than that of the sham group; no differences in brain water content were observed between the two groups in the contralateral basal ganglia (Cont-BG), ipsilateral cortex (Ipsi-CX), contralateral cortex (Cont-CX), or cerebellum (Cerebel) ($n = 6/\text{group}$, $*p < 0.01$ compared to sham group). (B) Hemispheric enlargement, determined by quantitative image analysis, was significantly greater in the ICH group than in the sham group ($n = 6/\text{group}$, $**p < 0.001$ compared to sham group). Values are means \pm SD.

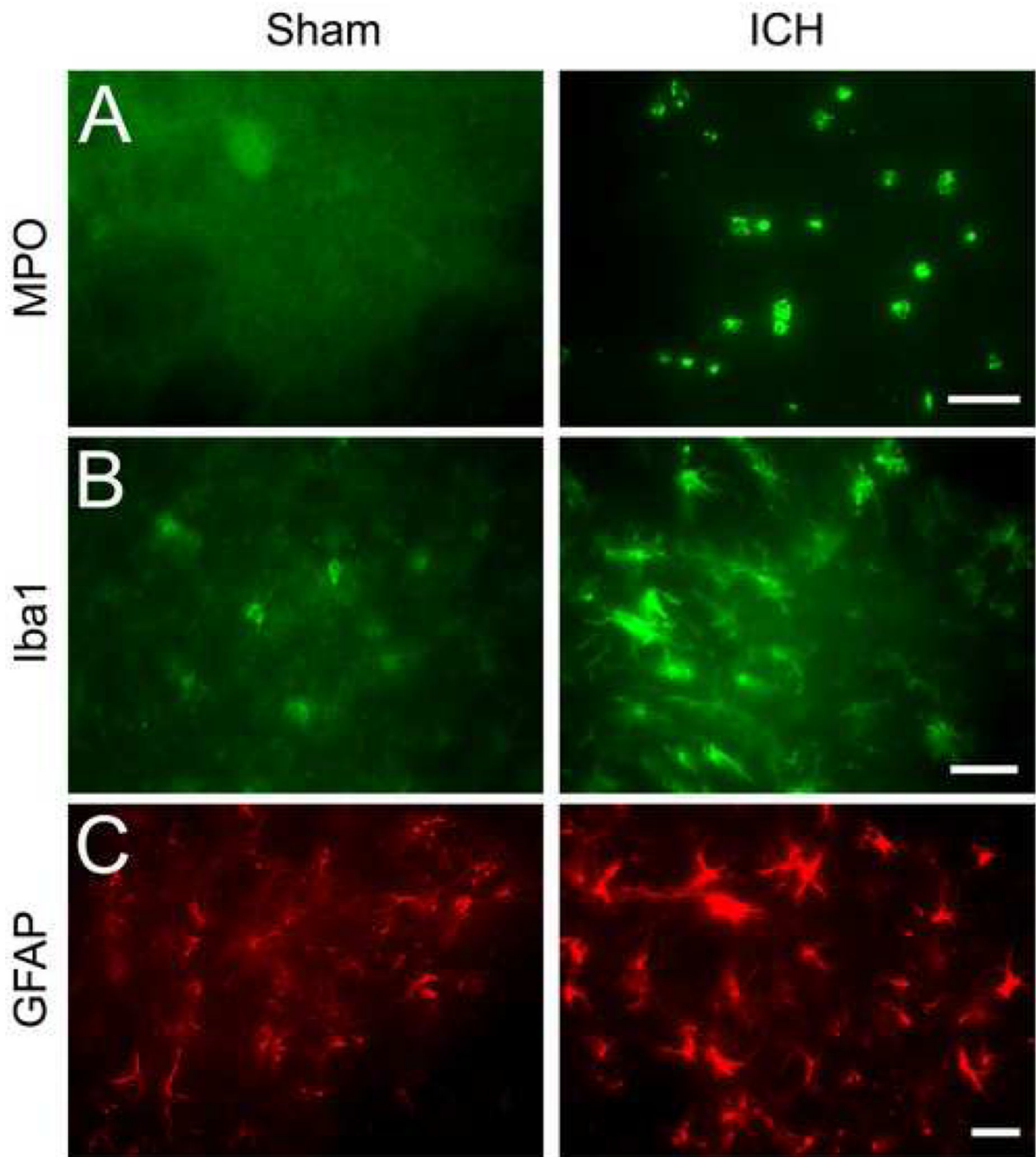


Fig. 4. The infusion of 10 μ l autologous whole blood into the striatum of mice produces a significant increase in neuroinflammation at 72 h. Age- and weight-matched C57BL/6 mice were randomly allocated into two groups: intracerebral hemorrhage group (ICH) and needle insertion only group (sham). (A) Infiltrating neutrophils (MPO-immunoreactive cells), (B) activated microglia/macrophages (Iba1-immunoreactive cells), and (C) reactive astrocytes (GFAP-immunoreactive cells) were apparent in or around the injury site in mice at 72 h; resting microglia/macrophages and astrocytes, but not infiltrating neutrophils, were observed

in the striatum of sham-operated control mice (all $n = 6/\text{group}$). Scale bar = 30 μm for A, B, C.

Author Manuscript

Author Manuscript

Author Manuscript

Author Manuscript

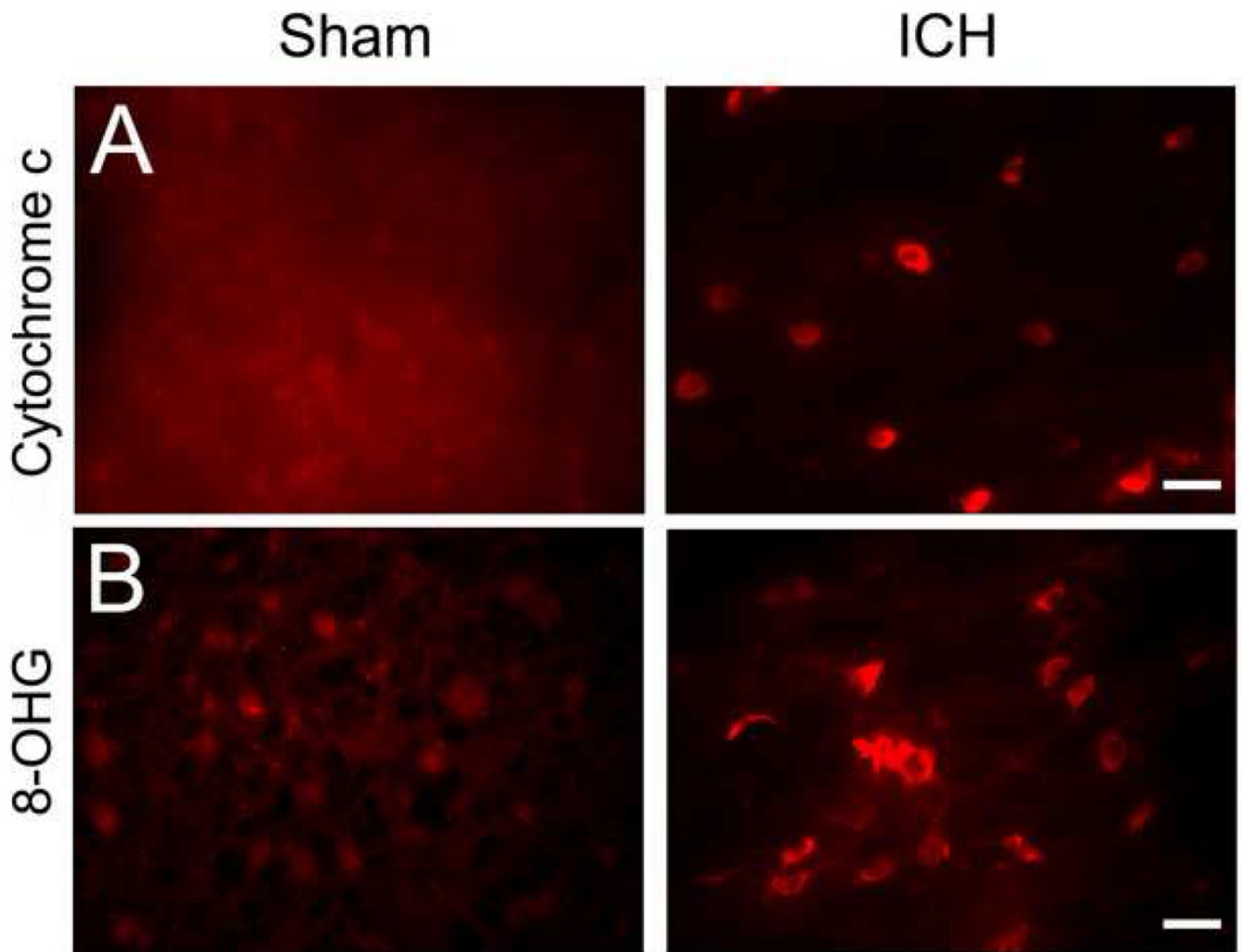


Fig. 5.

The infusion of 10 μ l autologous whole blood into the striatum of mice produces a significant increase in oxidative damage at 72 h. Age- and weight-matched C57BL/6 mice were randomly allocated into two groups: intracerebral hemorrhage group (ICH) and needle insertion only group (sham). (A) cytochrome c immunoreactivity, a marker for apoptosis, and (B) 8-hydroxyguanosine (8-OHG), a marker for DNA oxidation, were used to investigate oxidative damage after ICH. Immunoreactivity of cytosolic cytochrome c and 8-OHG was increased around the injury site 72 h after blood infusion but was not detected in the striatum of sham-operated control mice. Scale bar = 30 μ m for A and B. (both $n = 6$ /group).

Table 1

Mouse blood infusion models used in previous studies

Study	Blood origin	Anticoagulant used	Total blood infusion volume (infusion rate)
Belayev, et al., 2003	Donor blood from the heart	Heparin	15 µl; double infusion (5 µl /3 min, followed 7 min later by 10 µl/5min)
Nakamura, et al., 2004	Autologous blood from femoral artery	Not specified	30 µl; single injection (2 µl /min)
Tejima, et al., 2007	Autologous blood (No origin specified)	Not specified	20 µl; single injection (2 µl /min)
Xue, et al., 2006	Autologous blood from the tail	None	10 µl; single injection (3.3 µl /min)
Lee, et al., 2006	Autologous blood from tail vein	None	5 µl; single injection (1 µl /min)
Qu, et al., 2007	Autologous blood from tail vein	Heparin	15 µl; single injection (0.4 µl /min)
Zhao, et al., 2007	Autologous blood from femoral artery	Not specified	15 µl; single injection (3 µl /min)
Rynkowski, et al., 2008	Autologous blood from central tail artery or lateral tail veins	Heparin	30 µl; double infusion (5 µl /2.5 min, followed 7 min later by 25 µl /12.5 min)